Lines of Curvature for Polyp Detection in Virtual Colonoscopy

Lingxiao Zhao, Charl P. Botha, *Member, IEEE*, Javier O. Bescos, Roel Truyen, Frans M. Vos, and Frits H. Post

Abstract— Computer-aided diagnosis (CAD) is a helpful addition to laborious visual inspection for preselection of suspected colonic polyps in virtual colonoscopy. Most of the previous work on automatic polyp detection makes use of indicators based on the scalar curvature of the colon wall and can result in many false-positive detections. Our work tries to reduce the number of false-positive detections in the preselection of polyp candidates.

Polyp surface shape can be characterized and visualized using lines of curvature. In this paper, we describe techniques for generating and rendering lines of curvature on surfaces and we show that these lines can be used as part of a polyp detection approach. We have adapted existing approaches on explicit triangular surface meshes, and developed a new algorithm on implicit surfaces embedded in 3D volume data. The visualization of shaded colonic surfaces can be enhanced by rendering the derived lines of curvature on these surfaces.

Features strongly correlated with true-positive detections were calculated on lines of curvature and used for the polyp candidate selection. We studied the performance of these features on 5 data sets that included 331 pre-detected candidates, of which 50 sites were true polyps. The winding angle had a significant discriminating power for true-positive detections, which was demonstrated by a Wilcoxon rank sum test with $p < 0.001$. The median winding angle and inter-quartile range (IQR) for true polyps were 7.817 and $6.770 - 9.288$ compared to 2.954 and $1.995 - 3.749$ for false-positive detections.

Index Terms—Medical visualization, virtual colonoscopy, polyp detection, line of curvature, implicit surface.

1 Introduction

Colonic polyps are an important precursor of colon cancer, which is among the leading causes of cancer deaths in the western world [24]. A polyp is a benign growth of the colon lining. It typically presents as a sphere protruding from the colon wall. Early detection and removal of polyps significantly decrease the incidence of colon cancer. For this purpose, virtual colonoscopy has been developed as a procedure to inspect the interior wall of the human colon by using CT or MRI-scans.

Virtual colonoscopy is a minimally-invasive technique, which causes much less discomfort to the patient than traditional optical colonoscopy [3, 22]. The CT or MRI-scans are processed by iso-surface extraction or by direct volume rendering (DVR) to allow for visual inspection by a radiologist. However, a thorough, visual examination of the complete colon wall is rather time consuming, which makes the method unattractive for large-scale screening. Therefore, computer-aided techniques have been proposed to pre-detect and highlight colonic polyps in order to reduce the examination time and cost, especially in mass screening of low-incidence populations [26].

A considerable amount of work has been done in the field of automatic polyp detection; many schemes make use of curvature. Curvature is an important quantity from differential geometry [6], which is widely used in computer vision and visualization applications to characterize the shape of 3D surfaces. It can be represented by a scalar (e.g. mean or Gaussian curvature), and by two vectors, indicating the directions of principal curvatures at a given point.

Indicators based on scalar curvature values have been frequently used in previous work for computer-aided diagnosis (CAD) of colonic polyps. Yoshida et al. [33] made use of 3D geometric features called the volumetric shape index and curvedness to develop a CAD scheme for polyp detection. Näppi and Yoshida [18] proposed to use feature-guided analysis for achieving high sensitivity and a low false positive rate in their CAD scheme. Huang et al. [8] developed a two-stage curvature estimation method on triangular surface meshes and performed a filtering based on the sphericity index to identify potential polyps. Van Wijk et al. [31] introduced the technique of normalized convolution to measure curvature features in 3D volume data for automatic polyp detection. Accurate and noise-insensitive curvature calculation is essential for any such scheme. Representations based on point-sampling will in general be more sensitive to noise, whereas aggregation within a region of interest will enhance the robustness at the cost of some sensitivity. Using scalar curvature by itself for polyp detection can result in a large number of false-positive detections.

The potential of principal curvature direction fields has not yet been explored in current polyp detection techniques. On a surface, the two principal curvature directions define two orthogonal vector fields, and these can be visualized by *lines of curvature*, which are lines everywhere tangent to one of these vector fields. We will call these curves *streamlines of curvature*. They have also been used for surface shape analysis in engineering design [4]. However, to the best of our knowledge, no attempt has been made to apply streamlines of curvature for colonic polyp characterization in medical visualization. We hypothesize that the patterns in streamlines of curvature are a good indicator of specific features to detect polyps, both visually and automatically.

In our work, the proposed CAD process proceeds in three steps: pre-detection of polyp candidates, candidate selection, and finally enhanced visualization. Polyp candidates are pre-detected using an existing polyp detection scheme. These polyp candidates include many false-positive detections. The main contribution of our work is to propose a new additional polyp candidate selection approach based on a use of streamlines of curvature, which helps to reduce the number of false-positive detections. We will present methods to generate patterns of streamlines of curvature on the colon wall. We have improved existing algorithms for explicit triangle mesh surfaces, and developed a new method for implicit surfaces embedded in a 3D volume data representation. The basis of our work is a robust technique for the computation of principal curvature directions so that the streamlines

- *Lingxiao Zhao is with Data Visualization Group, Delft University of Technology, E-mail: zlx@graphics.tudelft.nl.*
- *Charl P. Botha is with Data Visualization Group, Delft University of Technology, E-mail: c.p.botha@tudelft.nl.*
- *Javier O. Bescos is with Philips Medical Systems Nederland BV, Best, E-mail: javier.olivan.bescos@philips.com.*
- *Roel Truyen is with Philips Medical Systems Nederland BV, Best, E-mail: roel.truyen@philips.com.*
- *Frans M. Vos is with Quantitative Imaging Group, Delft University of Technology and Dept. of Radiology, Academic Medical Centre, Amsterdam, E-mail: f.m.vos@tudelft.nl.*
- *Frits H. Post is with Data Visualization Group, Delft University of Technology, E-mail: frits.post@ewi.tudelft.nl.*

Manuscript received 31 March 2006; accepted 1 August 2006; posted online 6 November 2006.
For information on obtaining reprints of this article, please send e-mail to: tvcg@computer.org.

1077-2626/06/$20.00 © 2006 IEEE Published by the IEEE Computer Society

are as smooth as the surface itself. Subsequently, we ensure that a streamline accurately traces the true principal curvature directions of the surface. Note that constraining the streamlines to the surface will require extra operations compared to unconstrained streamline generation in a 3D vector field. For a good view of the local surface shape, a set of streamlines with controlled spacing must be generated, to reveal the important shape features, and to cover all important details. Therefore, the seeding and spacing of the streamlines is governed by local surface curvature. We extract features strongly correlated with true-positive detections from the generated streamlines. These new features provide a new basis for an automatic polyp detection algorithm. The streamlines of curvature support the perception of surface morphology in addition to the traditional shading. The shape is summarized using the streamlines that have specific patterns at polyp positions.

The rest of the paper is organized as follows. A brief survey of relevant research is given in section 2. In section 3, a relation between principal curvature directions and polyp surface characteristics is established. In section 4, our approach to generate surface-constrained streamlines of curvature and the seeding strategy is described. We start with an improvement of the existing algorithm on triangle meshes and then we describe a new scheme based on implicit iso-surfaces. The performance and applicability of these two methods are compared. In section 5, new features are defined on streamlines of curvature and used to select true-positive polyp detections. An experimental study of our polyp selection scheme and enhanced visualization of the colon wall are given in section 6. At the end of the paper, we draw some conclusions and suggest items for future work.

2 Related Research

Our work is related to many other research fields. The main purpose is to generate and render streamlines of curvature on the colonic surface and use them for improving automatic pre-detection of polyps.

Drawing from computer vision and visualization, surface curvature estimation is the basis of our curvature streamline generation. Triangle meshes are problematic for surface curvature estimation. We often do not have an analytical function describing the continuous surface approximated by the mesh. Concepts in differential geometry are no longer applicable in this discrete case. Approaches have been developed to approximate original surface curvature [27]. Mesh quality significantly influences the estimation results. Current triangle mesh extraction techniques often introduce strong artifacts. Most estimation methods suffer from mesh irregularities and data noise. Computing curvature directly from 3D volume data is based on derivatives of 3D images. These derivatives are usually estimated using kernel methods [30]. Parameters of the kernel must be properly set to achieve accurate and reliable results [5].

For triangle meshes, some methods [12] fit an analytic surface to a neighborhood of a mesh vertex and calculate curvature from the fitted function. Other methods estimate curvature for a surface region using total curvature defined in [19]. Lin and Perry [13] used the angle deficit to measure the Gaussian curvature. Meyer et al. [15] defined discrete differential geometry operators on triangle meshes. Taubin's method [28] is unique among other methods. It calculated curvatures at mesh vertices using the curvature tensor. For implicit iso-surfaces in 3D volume data, Thirion and Gourdon's method [29] was based on the implicit surface representations defined in differential geometry. The Hessian matrix of 3D volume data was introduced as another tool in [16].

Lines are often used to express shape features. Reflection lines on surfaces give designers crucial feedback on the quality of their product [21]. Interrante et al. [9] made use of line textures to enhance the perception of surface shape. In [1], streamlines in 2D optical flow were used to examine interesting features for polyp detection.

Streamlines of curvature can be traced on the surface and should be well distributed for efficient shape characterization. Nagy et al. [17] presented an interactive technique based on streamlines of curvature in 3D volume. Girshick et al. [7] introduced a simple scheme to trace streamlines of curvature on triangle meshes. In their work, streamlines were evenly spaced by using a special seeding method [11]. Mebarki et al. [14] proposed a fast farthest point seeding algorithm that can trace longer streamlines in 2D vector fields. Other work made use of local surface features to control the streamline density. Verma et al. [32] discussed characteristics of a good seeding strategy and presented a method using local flow topology. Alliez et al. [2] applied streamlines of curvature for surface remeshing. They traced streamlines in the parameter space of a surface after the original surface was flattened. Curvatures were employed to optimize the streamline density in order to preserve surface information after remeshing. However their work did not apply to implicit iso-surfaces.

3 Polyp Characterization Using Lines of Curvature

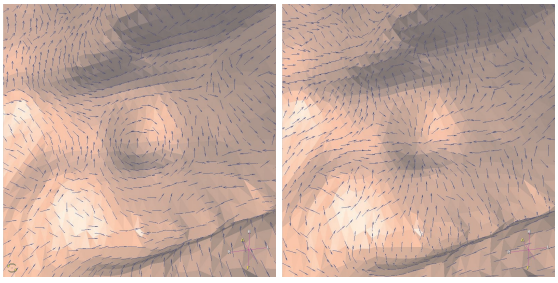

Fig. 1. Distinctive patterns on polyp surfaces. Left: Circular pattern in maximum curvature directions. Right: Focusing pattern in minimum curvature directions.

The idea of using streamlines of curvature for polyp candidate selection is inspired by visualizing the two vector fields of surface principal curvature directions. Our work starts with curvature estimation on triangular surface meshes, both for scalar curvature and for principal curvature directions.

A robust curvature estimation approach, named the Normal Vector Voting (NVV) method [20], is applied on triangular colonic surfaces extracted from real CT scans using Marching Cubes. We will discuss the NVV method later in Section 4.1. Visual inspection of principal curvature directions shows patterns on polyp surfaces that may discriminate polyps from healthy tissue (Figure 1). In the case that mesh surface normals point towards the interior of the colon, the maximum curvature directions around the polyp present a circular pattern while the minimum curvature directions present a focusing pattern. This relation can be explained with a generalization of the polyp surface.

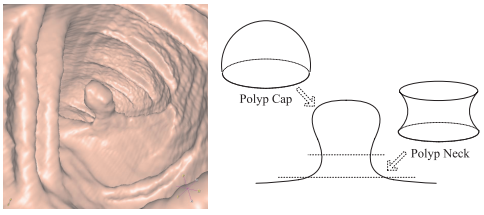

Fig. 2. A polyp surface has two parts: ideally, the cap is spherical and convex, the neck is a closed-ring and anticlastic surface.

A polyp surface consists of two parts, the top part and the bottom part (Figure 2). We call the top part the polyp cap and the bottom part the polyp neck. The polyp cap is the most protruding area on a polyp surface. It is ideally represented as a spherical or ellipsoidal surface. The polyp neck is the transition area from the background to the polyp cap. It is typically a closed-ring and anticlastic surface, i.e. all points on the polyp neck are hyperbolic. Considering the local geometric properties, surface principal curvature directions on the polyp cap do not always show characteristic patterns. Sometimes, a polyp can not be easily identified only according to its cap. Most existing polyp detection methods use indicators based on scalar curvatures, e.g. the volumetric shape index [33] and the sphericity index [8]. Such indicators only work on the polyp cap. Therefore, they sometimes can

introduce many false-positive detections. The polyp neck is a distinctive part of the polyp. Every polyp has a neck as long as it protrudes from the colon wall. Around such an anticlastic area, principal curvature directions present particular patterns of polyps, i.e. circular or focusing patterns.

Streamlines of curvature can be used to visualize principal curvature directions on the colonic surface. Therefore, specific patterns in streamlines of curvature can help to discriminate polyps from background. The circular pattern in maximum curvature directions around the polyp neck suggests potential. Since the polyp neck is typically a closed-ring area, approximately closed streamlines are expected to locally represent the polyp narrow part or neck. For this reason, we propose to supplement existing polyp detection methods with an analysis on the polyp neck.

4 Generating and Rendering Lines of Curvature on Colonic Surfaces

Streamlines of curvature support polyp candidate selection and enhance polyp visualization when they are superimposed on the colon wall. This section describes techniques to generate these curves on explicit triangle meshes as well as on implicit iso-surfaces.

4.1 Lines of Curvature on Explicit Triangle Mesh Surfaces

The first step to generate streamlines of curvature on triangle meshes is curvature estimation. Smooth and regular principal curvature directions are desired to correspond with surface shape. The NVV method developed by Page et al. [20] is a robust curvature estimation approach on general triangle meshes even with low quality. It uses the geodesic neighborhood as an improvement of other types of neighborhoods, e.g. the k-ring ($k = 1,2,3,\ldots$) neighborhood. It is defined to be a surface region bounded by a user-specified geodesic distance from the central mesh vertex. A k-geodesic neighborhood not only enlarges the computation area but also supports balanced directional sampling around a mesh vertex. This is very useful to reduce the effects of mesh irregularity and noise.

The NVV method provides robust curvature estimation on triangle meshes, for both scalar curvature values and principal curvature directions. We extended and improved the streamline tracing technique described in [7] on triangular colonic surfaces, by integrating the NVV method and a simplified computation. This algorithm traces the streamline on the mesh by projecting each integration onto the local mesh triangle. When the streamline reaches a mesh edge, the intersection point with that edge is added and the local mesh triangle is updated. We found calculating intersection points of mesh-constrained streamlines and edges to be complicated by the limited floating point precision. The inaccuracy caused by this accumulates as an error during streamline integration. To alleviate this problem and simplify the computation of intersection points, we transform the problem to 2D. We define a local 2D coordinate system for each triangle plane. A triangle vertex is set to be the origin. One axis coincides with a triangle edge. Intersections with edges can be easily computed in this 2D coordinate system and then transformed to 3D.

We characterize the local surface shape using collections of streamlines. Therefore it is important that streamlines of curvature are distributed regularly over the triangle mesh using a seeding strategy. The evenly distributed streamlines in [7] may lose details of surface shape. An adaptive and efficient way was presented in [2]. Although the application is different, curvature controlled seeding contributes much to polyp surface characterization. Streamlines of curvature on a colonic surface mesh are shown in Figure 3. In this case, the appearance and accuracy of streamlines are significantly affected by the mesh quality and estimated principal curvature directions.

4.2 Lines of Curvature on Implicit Iso-surfaces

Implicit surfaces are widely used in Virtual Colonoscopy. Compared to an explicit triangle mesh, an implicit surface provides a smoother and clearer visualization of the colon wall.

An implicit surface is embedded in a 3D volume as an iso-surface. It is usually visualized using volume ray casting techniques. In this section, we describe a new approach to generate streamlines of curvature on implicit iso-surfaces. We first discuss iso-surface curvature estimation. Then we describe our curvature streamline tracing on implicit iso-surfaces. We have adapted the strategy of curvature controlled seeding and spacing for this case.

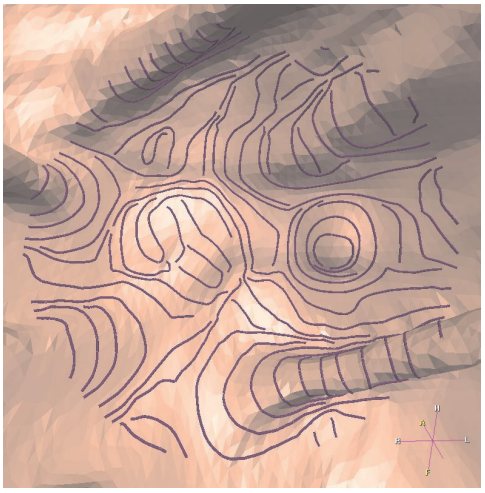

Fig. 3. Streamlines of maximum curvature are generated and rendered on the triangular colonic surface.

4.2.1 Curvature Estimation on Iso-surfaces

We use the method proposed by Van Vliet and Verbeek [30] to estimate principal curvatures on an iso-surface in 3D volume data. There are three steps in this algorithm.

First, we calculate the gradient vector $\mathbf{g}$ and the Hessian matrix $\mathbf{H}$ at a position $\mathbf{P}$ on the iso-surface in 3D volume based on the following definitions:

$$\mathbf{g} = (f_x, f_y, f_z) \qquad \mathbf{H} = \begin{pmatrix} f_{xx} & f_{xy} & f_{xz} \\ f_{xy} & f_{yy} & f_{yz} \\ f_{xz} & f_{yz} & f_{zz} \end{pmatrix}$$

Entries in these definitions are partial derivatives of the 3D image:

$$f_x = \frac{\partial f}{\partial x} \qquad \text{and} \qquad f_{xx} = \frac{\partial^2 f}{\partial x^2}$$

These derivatives can be estimated in a 3D volume by convolution with the derivative of a Gaussian function with a specific kernel width σ.

Second, the Hessian matrix $\mathbf{H}$ is rotated to align one axis with the local gradient direction $\mathbf{g}$. The rotated Hessian matrix can be written as:

$$\mathbf{H_r} = \begin{pmatrix} f_{gg} & \cdots & \cdots \\ \vdots & f_{uu} & f_{uv} \\ \vdots & f_{uv} & f_{vv} \end{pmatrix} = \begin{pmatrix} f_{gg} & \cdots \\ \vdots & \mathbf{H_t} \end{pmatrix}$$

where f_{gg} is the second order derivative along the gradient direction, u and v are the other two axes in the local coordinate system and $\mathbf{H_t}$ is a 2D Hessian matrix in the plane uv.

Finally we perform eigen analysis on the 2D $\mathbf{H_t}$. Local principal curvature values at $\mathbf{P}$ can be computed based on the local gradient magnitude and two eigenvalues λ_1 and λ_2:

$$k_1 = \frac{-\lambda_1}{\|\mathbf{g}\|} \qquad \text{and} \qquad k_2 = \frac{-\lambda_2}{\|\mathbf{g}\|}$$

The two eigenvectors correspond to principal directions in the tangent plane uv at $\mathbf{P}$. They must be transformed to the original 3D coordinate system.

Since most 3D CT images involve noise, we must choose a proper Gaussian convolution kernel width σ. In our implementation, σ is set to be 2.0 millimeters and kernel size is 11 voxels with regard to covering noise and computational efficiency.

4.2.2 Tracing Lines of Curvature on Implicit Iso-surfaces

Tracing a streamline of curvature on an implicit iso-surface is different from a triangle mesh. The position of the surface is not explicitly known. The work in [7, 17] also included approaches tracing streamlines of curvature in 3D volume. But such streamlines are not constrained to iso-surfaces. In our approach, we restrict streamline points to the iso-surface in an implicit way when tracing through the 3D volume.

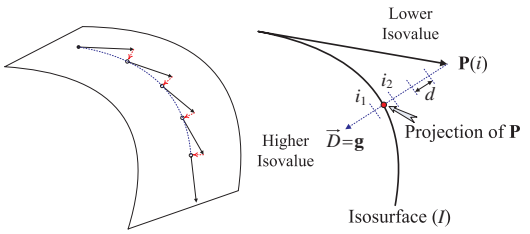

Fig. 4. Left: Streamline tracing on iso-surfaces. Right: Projection of initially integrated point on iso-surfaces.

A streamline is traced using stepwise integration from a seed point in forward and reverse directions. For each integration step, first we calculate principal curvature directions at the current streamline point on the iso-surface using the method in Section 4.2.1. Currently we use linear interpolation to estimate the gradient, the Hessian and the data value at an arbitrary position in the 3D volume. Higher order interpolation, e.g. cubic interpolation, may give a better result. Then the streamline is propagated one step further following the local principal curvature direction. This is a first order integration and higher order schemes, e.g. second and fourth order Runge-Kutta methods, are other improvements. Higher order interpolation will work better only with higher order integration. Since the principal curvature directions are tangents to the iso-surface at the current point, the next point initially integrated in first order generally is not on the iso-surface (See Figure 4). Therefore, we project it back onto the iso-surface. First, the gradient vector $\mathbf{g}$ and data value i are calculated at the initial point $\mathbf{P}$. If i is smaller than the isovalue I of the implicit iso-surface, the projection direction $\vec{D}$ is $\mathbf{g}$. Otherwise, $\vec{D}$ is $-\mathbf{g}$. Then we iteratively move $\mathbf{P}$ along $\vec{D}$ for a step length d and compute i at $\mathbf{P}$ after each step. i_1 and i_2 are defined to be two consecutive values of i. If one of them is smaller than I and the other is larger, we stop this procedure and compute $\mathbf{P}'$ as the projection of $\mathbf{P}$ on the implicit iso-surface using:

$$\mathbf{P}' = \mathbf{P} - \left(\frac{i_1 - I}{i_1 - i_2} \cdot d\right) \cdot \vec{D}$$

Streamline tracing and projection on implicit iso-surfaces are explained in Figure 4. A reasonable value for the projection step length d is $\frac{1}{20} \times VoxelLongestDiagonal$, where $VoxelLongestDiagonal$ is the longest diagonal of a volume voxel. If we use a very small step length in first order integration or use the fourth order Runge-Kutta method to trace a streamline in 3D volume, this projection technique may not be necessary.

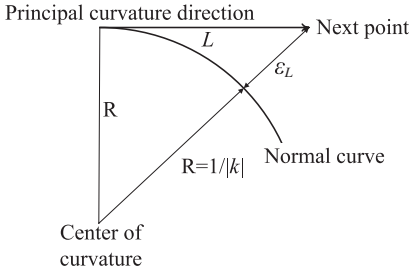

Fig. 5. Use curvatures to adapt streamline integration step length on iso-surfaces.

On a highly curved surface area, a long streamline integration step may miss important surface information. This can be improved by using the surface curvature to adapt the step length. We developed the approach shown in Figure 5. The osculating circle is used to approximate the relative local iso-surface normal curve. When tracing in a principal curvature direction, the integration step length L is dependent on the corresponding curvature value k:

$$L = \sqrt{\varepsilon_L \left(\frac{2}{|k|} + \varepsilon_L\right)}$$

where ε_L is specified by the user to bound the distance how far the point is allowed to move away from the iso-surface. Our implementation sets $\varepsilon_L = \frac{1}{10} \times VoxelLongestDiagonal$. We also specify a longest step length $L_{max} = 0.3mm$ when tracing on a flat surface area.

4.2.3 Curvature Controlled Seeding on Implicit Iso-surfaces

We modified the curvature-adapted seeding strategy in [2] to distribute streamlines on implicit iso-surfaces. The basic idea of using curvatures to control streamline density on surfaces is to use minimum curvature value to determine the spacing distance between streamlines following maximum curvature direction, and vice versa. We follow a procedure similar to the evenly spaced seeding [11]. We first start a streamline from a chosen point on the surface. For each integration step of tracing, a pair of new seeds placed perpendicularly to the integration segment at the local curvature controlled spacing distance (Figure 6) is put into a seed queue. Then we iteratively pick another seed in the seed queue and start another new streamline. Except for the first streamline, every time a new streamline is generated, we must remove invalid seeds from the queue before new valid seeds are added. This seeding procedure stops when there is no valid seed. A seed is valid if the distance between it and any streamline point is not less than its local curvature controlled spacing distance. A streamline stops when it is too close to other streamlines or reaches a certain maximum number of integrations.

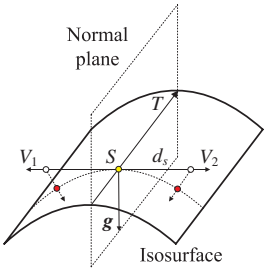

Fig. 6. A pair of seeds is initially placed perpendicularly to each streamline segment. Then they are projected onto the iso-surface.

We developed a method to place the seed on the implicit iso-surface. For each streamline integration (Figure 6), we initially place a pair of seeds perpendicular to the current streamline segment on the local tangent plane. At every streamline point S, we construct a normal plane containing the streamline integration direction T and the local gradient vector $\mathbf{g}$. We then compute two vectors V_1 and V_2, orthogonal to and pointing outwards from the normal plane:

$$V_1 = T \times G \qquad \text{and} \qquad V_2 = G \times T$$

The next problem is to decide the spacing distance d_s to place the initial seeds along V_1 and V_2. In the case shown in Figure 7, the distance from the initial seed point to the iso-surface is bounded by ε_1. Then the spacing distance d_s will be specified based on the controlling curvature k:

$$d_s = \sqrt{\varepsilon_1 \left(\frac{2}{|k|} + \varepsilon_1\right)}$$

These two initial seeds generally are not exactly on the iso-surface. Therefore they are projected using the projection technique described in Section 4.2.2.

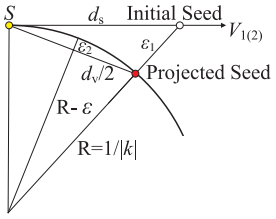

Fig. 7. Use curvatures to control streamline spacing distance and seed validating distance.

Invalid seeds in the potential seeds queue are removed after a new streamline is traced. To validate a seed, we specify another error boundary ε_2. In Figure 7, an osculating circle approximates the intersection arc of the iso-surface between the local streamline point S and a seed on the iso-surface. The optimal spacing distance between these two points is the arc length. The Euclidean distance is used as an approximation to simplify the computation. Its path is offset from the circle arc by a small distance. This distance is bounded by ε_2. Thus the local curvature controlled spacing distance is dependent on the controlling curvature k:

$$d_v = 2 \times \sqrt{\varepsilon_2 \left(\frac{2}{|k|} - \varepsilon_2 \right)}$$

d_v can also be used to validate when to stop the tracing of a streamline. As ε_2 can be computed based on ε_1, we only need to specify one error boundary ε_1:

$$\varepsilon_2 = \frac{1}{|k|} \left(1 - \sqrt{\frac{2+|k| \times \varepsilon_1}{2 \times (1+|k| \times \varepsilon_1)}} \right)$$

In our experiments, $\varepsilon_1 = \frac{1}{10} \times VoxelLongestDiagonal$ yielded the best result.

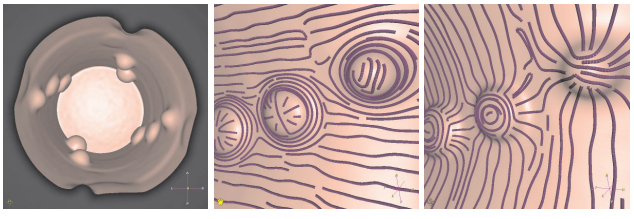

Fig. 8. Streamlines of curvature on the implicit iso-surface embedded in an artificial 3D volume. Left: A synthetic colon model with many polyp-like bumps. Central: streamlines of maximum curvature. Right: streamlines of minimum curvature.

When tracing in one principal curvature direction, the controlling curvature k corresponds to the other principal curvature direction. Figure 8 shows the results of our algorithm on an artificial 3D volume data. On both triangle meshes and implicit iso-surfaces, a streamline of curvature is rendered as a polyline. In order to make a streamline more visible, a thin tube is rendered around it.

4.3 Comparison

We compared our two techniques described to generate streamlines of curvature on triangle meshes and implicit iso-surfaces. We only focused on the streamline tracing and spacing. Surface curvature estimation was performed as part of the preprocessing stage and we assumed comparable and robust curvature estimations in both cases. Linear interpolation and first order integration were used. We tested on both synthetic data sets and real data sets. Our workstation had a 2.60GHz Pentium 4 CPU with 1GB of memory. The graphics card was NVIDIA GeForce4 MX440 with 64MB.

We first recorded computation time in each implementation. Nine synthetic data sets and five real data sets were used. Streamlines were generated for each detection patch with a radius of 16 millimeters.

Table 1. Comparison of Computation Time: Streamlines are generated per detection patch.

	triangle meshes	Iso-surfaces
Average Number of Streamlines	43.3	41.2
Average Number of Points	1781	1072
Average Computation Time (sec.)	6.60	3.78

Spacing distance between streamlines was less than 2 millimeters. Table 1 gives a first result for both techniques. It indicates that our technique applied to implicit iso-surfaces offers a faster computation for streamline tracing and spacing on a certain part of a surface. The main reason is that mesh-constrained streamlines have more integrations including many intersections with mesh edges.

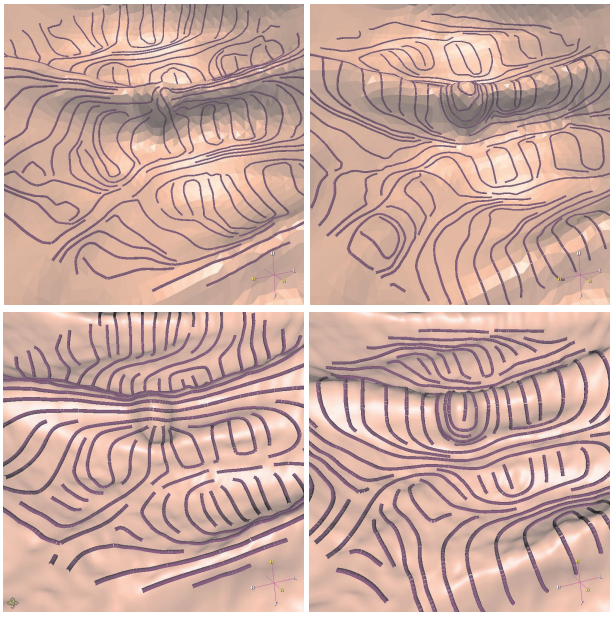

Fig. 9. Comparison of curvature streamline appearance on the triangle mesh and the iso-surface of a medical 3D volume data: Left two show streamlines of minimum curvature, right two show streamlines of maximum curvature.

Another comparison criterion was the appearance of the streamlines. Since we want to use streamlines of curvature as a tool to characterize specific features of polyps, the shape of the streamline is most important. In Figure 9, streamlines of curvature are generated on a triangle mesh and an iso-surface in a real medical data. This 3D volume data is $512 \times 512 \times 255$. Judged by visual inspection, our technique for implicit iso-surfaces gives better results. Streamlines in this case appear to be smoother, longer and more characteristic.

Both triangle meshes and implicit iso-surfaces offer relative advantages in different visualization applications. These two different techniques should be employed on corresponding surface representations. If both of them are applicable, the technique for implicit surfaces is preferred. It favors our improved CAD process in virtual colonoscopy.

5 Feature Calculation on Lines of Curvature

Streamlines of curvature with specific patterns, i.e. (almost) closed streamlines, are inspected around the polyp neck. The polyp neck can be identified by detecting such characteristic curves on the colonic surface. To do this, we generate streamlines of curvature for each predetected polyp candidate area and select streamlines on each polyp neck. Then we calculate features on the selected streamlines to detect specific patterns.

5.1 Selecting Lines of Curvature on the Polyp Neck

We generate collections of streamlines on the colonic surface. Only those streamlines presenting distinctive patterns characteristic of the

polyp neck are used for the diagnosis, others may even confuse the result.

We present a method to automatically select important streamlines. In our case, we are most interested in streamlines on the polyp neck area. We combined the use of curvature magnitudes with streamline selection. Considering the fact that the polyp neck area is an anticlastic surface (Section 3), the two principal curvature values everywhere on such a surface have opposite signs. In other words a streamline generated around the polyp neck should have many hyperbolic points. We define a quantity, named hyperbolic percentage HP, as a feature to select streamlines on the polyp neck:

$$HP = \frac{n_h}{N} \times 100\%$$

where n_h is the number of hyperbolic points and N is the total number of points on a streamline. A hyperbolic point on the surface has principal curvature values with opposite signs.

The HP is computed for each streamline generated. Then we select the first $\mathbf{N}$ streamlines with the largest n_h. Each selected streamline must have a $HP \geq 50\%$. Our experience shows that $\mathbf{N} = 3$ or 5 offers simplified computation and guarantees that streamlines on the polyp neck are always selected.

5.2 Calculating Streamline Features for Polyp Characterization

We want to find (almost) closed streamlines of maximum curvature in the region of the polyp neck. Therefore, our problem seems to be the topic of detecting (almost) closed streamlines on 3D surfaces.

The detection of specific patterns of streamlines, e.g. closed streamlines and swirling streamlines, is a topic in flow visualization techniques. Our polyp candidate selection scheme is similar to the detection of flow vortices using streamlines. In 2D flow fields, Portela [23] introduced the winding angle of streamlines to detect vortices. Sadarjoen et al. [25] proposed to use the sum of signed angles along a streamline as a simplification. In 3D cases, winding angles are no longer meaningful. Portela [23] suggested reducing the problem from 3D to 2D by projecting local vectors onto the swirl plane. Jiang et al. [10] presented an algorithm to detect swirling features based on the geometry of streamlines.

Swirling streamline patterns used to detect vortices in fluid flow are different from the curvature line patterns to detect polyps. We want to find (almost) closed streamlines, but we can use similar techniques such as the winding-angle technique [25]. In 2D flow fields, the winding angle is defined as the cumulative change of direction of the streamline segments. It measures the rotation of a streamline. A swirling streamline must have a winding angle of at least 2π. This feature is used to detect swirling patterns of vortices in 2D flow fields. However the winding angle is inherently limited to 2D.

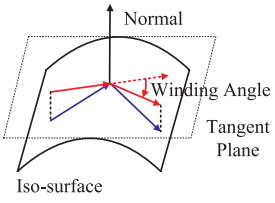

Fig. 10. Adapt the winding angle method: the changing angle of streamline direction is projected onto the local tangent plane.

We generalized the winding angle concept to space curves. Since streamlines of curvature are traced on 3D colonic surfaces, surface normals could be obtained at streamline points. For each streamline point, the changing angle of streamline direction is projected onto the local tangent plane (Figure 10). This projected angle is signed according to the right-hand rule. The sum of such signed angles along a closed streamline may be less than 2π. Therefore, a streamline is considered to be closed if it has two points within a certain very small distance from each other, however the arc length of the streamline in between should be above a certain threshold. The winding angle is computed for each selected streamline, and then the largest winding angle is used as an important feature per pre-detected polyp candidate.

Only polyps larger than $5mm$ in diameter are significant for clinical diagnosis. There are also small bumps on the colon wall, which are not real polyps. Our streamline generation algorithm also generates (almost) closed streamlines around them. To separate them from true polyp detections, we also measure the size of the area enclosed by the (almost) closed streamline in terms of the mean radius. The mean radius of a closed streamline is defined as the average distance from the mean center of the streamline to its points. The mean radius of the selected streamline that has the largest winding angle is used as an additional feature per candidate area in our polyp candidate selection.

6 Results

In this section we document the results of a study that we performed on 5 patient data sets to demonstrate the utility of our streamline selection and streamline-based feature calculation for polyp detection strategies. We also show renderings which illustrate how our surface-constrained curvature streamlines enhance the visual perception of colonic surface shape in virtual colonoscopy.

6.1 Polyp Candidate Selection Study

We are planning to integrate our streamline selection and streamline-based feature calculation in a complete polyp detection protocol. The first stage of the protocol is a polyp pre-detection phase [33] that yields all true-positive detections (as confirmed by medical diagnosis), and also a large number of false-positive detections. Suspect locations are first detected on the colonic surface based on the volumetric shape index. During the second stage, the number of false-positive detections will be reduced using various classification techniques.

We assessed the value of our streamline selection and the winding angle calculation to discriminate between true- and false-positive polyp detections in a large number of candidate areas, with the goal of integrating these techniques in the second stage of polyp detection and classification. CT scans were performed on five patients with a Philips Mx8000 multislice scanner. The average voxel size of the 3D volume image is $0.77mm \times 0.77mm \times 1.60mm$. The preprocessing algorithm [33] detected 331 polyp candidate areas in total. An expert opinion of an experienced radiologist was used to classify these candidate areas into true- and false-positive detections, where true-positive detection indicates a definite polyp and false-positive detection a non-polyp. Of the 331 candidate areas, 50 sites (15.1%) were classified as true-positive detections. True-positive detections were found in all 5 patients.

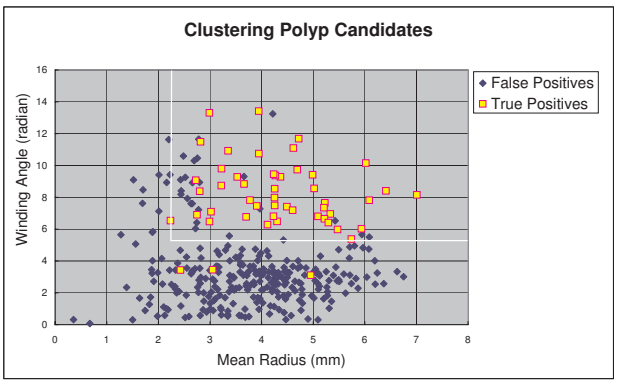

Fig. 11. Features of Streamlines: Mean Radius and Alternative Winding Angles. True- and false-positive detections are visually clustered.

We applied our streamline selection and winding angle calculation method on all 331 candidate areas. The winding angle was significantly higher for true-positive detections than for false-positive detections (Wilcoxon rank sum test, $p < 0.001$). The median winding angle and inter-quartile range (IQR) for the true-positive detections was 7.817 and 6.770–9.288 compared to 2.954 and 1.995–3.749 for the

false-positive detections. Figure 11 shows clustering of the true- and false-positive detections. These results indicate that streamline selection and winding angle measurements in candidate areas could make a valuable contribution to an approach for discriminating between true- and false-positive polyp candidate areas as detected by the preprocessing algorithm.

6.2 Enhanced Visualization

The visualization of the shaded colon wall can also benefit from streamlines of curvature (images on the left of Figure 12). This can greatly enhance the perception of colonic surface features, e.g. polyps. We also show the results of our automatic streamline selection method in the images on the right of Figure 12. As can be seen in these images, one or more of the selected streamlines are situated on the polyp neck.

7 Conclusions and Future Work

Our work explored the potential of surface principal curvature directions to characterize specific surface shape features, e.g. colonic polyps in virtual colonoscopy. Streamlines of curvature were used to visualize such vector fields. The most important elements are robust methods for curvature calculation, surface-constrained streamline integration, and the use of adaptive seeding and spacing of the streamlines. We developed a new scheme for curvature controlled spacing of streamlines on implicit iso-surfaces. Both the implicit and explicit surface implementations showed good results for surface curvature streamlines. In particular, our approach is useful for implicit surface characterization based on 3D volume data.

(Almost) closed streamlines can be generated on the polyp neck area. Therefore we expect that such characteristic patterns are a good indicator of colonic polyps in virtual colonoscopy. Streamlines are selected based on the local surface geometry and new features are calculated on selected streamlines. A statistical analysis indicated that such streamline features are highly correlated with true-positive detections of a preprocessing polyp detection method. The polyp neck area is considered as an addition to the polyp cap, which is often the main focus of current polyp detection techniques. Our newly defined features on curvature streamlines are expected to reduce the number of false-positive polyp candidates in a pre-detection. We proposed a new polyp candidate selection scheme that can be easily combined with other techniques to improve current computer-aided detection. An enhanced visualization of the colon wall by curvature line patterns can also improve the perception of colonic surface shape for radiologists.

There are a number of promising avenues for future research towards a robust polyp detection technique. For the techniques described, the use of higher order integration and interpolation methods can possibly lead to more accurate results. The streamline-enhanced visualization must be compared with the standard visualization in a clinical environment. Our polyp candidate selection scheme will also be tested with a large number of clinical CT scans to obtain a generalized specification of its performance.

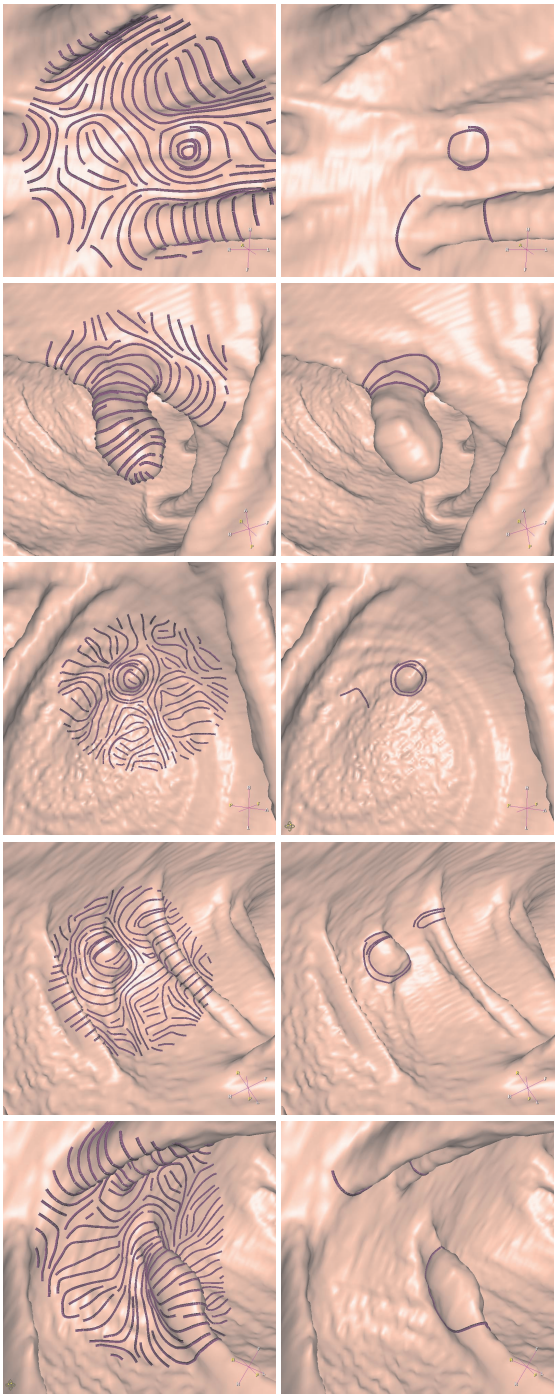

Fig. 12. Images on the left: The perception of colonic surface shape is enhanced using streamlines of curvature; Images on the right: Streamlines are automatically selected using the algorithm described in Section 5.1, one or more of the selected streamlines are situated on the polyp neck area.

Acknowledgements

This work is supported in part by Philips Medical Systems Nederland BV, Best, the Netherlands. The authors thank Dr. Frans A. Gerritsen and Ir. C. van Wijk for kind advices and helpful discussions, as well as providing the authors with CT scans of patients.

References

[1] B. Acar, S. Napel, D. Paik, B. Göktürk, C. Tomasi, and C. F. Beaulieu. Using optical flow fields for polyp detection in virtual colonoscopy. In *Lecture Notes in Computer Science: Proceedings of the 4th International Conference Medical Image Computing and Computer-Assisted Intervention (MICCAI)*, volume 2208, pages 637–644, Oct. 2001.

[2] P. Alliez, D. Cohen-Steiner, O. Devillers, B. Lévy, and M. Desbrun. Anisotropic polygonal remeshing. *ACM Transactions on Graphics (Proceedings of ACM SIGGRAPH 2003)*, 22(3):485–493, July 2003.

[3] D. Bartz. Virtual endoscopy in research and clinical practice. *Computer Graphics Forum*, 24(1):111–126, Mar. 2005.

[4] J. M. Beck, R. T. Farouki, and J. K. Hinds. Surface analysis methods. *IEEE Computer Graphics and Applications*, 6(12):18–36, Dec. 1986.

[5] S. R. Campbell and R. M. Summers. Analysis of kernel method for surface curvature estimation. In *International Congress Series*, volume 1268, pages 999–1003, 2004.

[6] M. D. Carmo. *Differential Geometry of Curves and Surfaces*. Prentice-Hall, Englewood Cliffs, NJ, 1976.

[7] A. Girshick, V. Interrante, S. Haker, and T. Lemoine. Line direction matters: an argument for the use of principal directions in 3D line drawings. In *Proceedings of First International Symposium on Non-Photorealistic Rendering*, pages 43–52, 2000.

[8] A. Huang, R. M. Summers, and A. K. Hara. Surface curvature estimation for automatic colonic polyp detection. In *Medical Image 2005: Physiology, Function and Structure from Medical Images, Proceedings of SPIE*, volume 5746, pages 393–402, 2005.

[9] V. Interrante, H. Fuchs, and S. Pizer. Enhancing transparent skin surfaces with ridge and valley lines. In *Proceedings of IEEE Visualization 1995 (VIS'95)*, pages 52–59, 1995.

[10] M. Jiang, R. Machiraju, and D. Thompson. Geometric verification of swirling features in flow fields. In *Proceedings of IEEE Visualization 2002 (VIS'02)*, pages 307–314, Oct. 2002.

[11] B. Jobard and W. Lefer. Creating evenly-spaced streamlines of arbitrary density. In *Proceedings of the Eurographics Workshop on Visualization in Scientific Computing*, pages 45–55, 1997.

[12] P. Krsek, T. Pajdla, and V. Hlaváč. Estimation of differential parameters on triangulated surface. In *Proceedings of the Czech Pattern Recognition Workshop '97*, pages 151–155, Feb. 1997.

[13] C. Lin and M. J. Perry. Shape description using surface triangulation. In *Proceedings of the IEEE Workshop on Computer Vision: Representation and Control*, pages 38–43, 1982.

[14] A. Mebarki, P. Alliez, and O. Devillers. Farthest point seeding for efficient placement of streamlines. In *Proceedings of IEEE Visualization 2005 (VIS'05)*, pages 479–486, Oct. 2005.

[15] M. Meyer, M. Desbrun, P. Schröder, and A. H. Barr. Discrete differential-geometry operators for triangulated 2-manifolds. In *Proceedings of VisMath*, 2002.

[16] O. Monga, S. Benayoun, and O. D. Faugeras. From partial derivatives of 3D density images to ridge lines. In *Proceedings of IEEE Computer Society Conference on Computer Vision and Pattern Recognition*, pages 354–359, June 1992.

[17] Z. Nagy, J. Schneider, and R. Westermann. Interactive volume illustration. In *Proceedings of Vision, Modeling and Visualization Workshop (VMV)*, 2002.

[18] J. Näppi and H. Yoshida. Feature-guided analysis for reduction of false positives in CAD of polyps for computed tomographic colonography. *Medical Physics*, 30(7):1592–1601, July 2003.

[19] B. O'Neill. *Elementary Differential Geometry*. Academic Press, Orlando, FL, second edition, 1997.

[20] D. L. Page, Y. Sun, A. F. Koschan, J. Paik, and M. A. Abidi. Normal vector voting: crease detection and curvature estimation on large, noisy meshes. *Graphical Models*, 64(3/4):199–229, May/July 2002.

[21] N. M. Patrikalakis and T. Maekawa. *Shape Interrogation for Computer Aided Design and Manufacturing*. Springer, first edition, 2002.

[22] P. J. Pickhardt, J. R. Choi, I. Hwang, J. A. Butler, M. L. Puckett, H. A. Hildebrandt, R. K. Wong, P. A. Nugent, P. A. Mysliwiec, and W. R. Schindler. Computed tomographic virtual colonoscopy to screen for colorectal neoplasia in asymptomatic adults. *The New England Journal of Medicine (NEJM)*, 349(23):2191–2200, Dec. 2003.

[23] L. M. Portela. *Identification and Characterization of Vortices in the Turbulent Boundary Layer*. PhD thesis, Stanford University, 1997.

[24] J. D. Potter, M. L. Slattery, R. M. Bostick, and S. M. Gapstur. Colon cancer: a review of the epidemiology. *Epidemiologic Reviews*, 15(2):499–545, 1993.

[25] A. Sadarjoen and F. H. Post. Geometric methods for vortex extraction. In *Data Visualization, proceedings of VisSym 99*, pages 53–62, May 1999.

[26] R. M. Summers, J. Yao, P. J. Pickhardt, M. Franaszek, I. Bitter, D. Brickman, V. Krishna, and J. R. Choi. Computed tomographic virtual colonoscopy computer-aided polyp detection in a screening population. *Gastroenterology*, 129(6):1832–1844, Dec. 2005.

[27] T. Surazhsky, E. Magid, O. Soldea, G. Elber, and E. Rivlin. A comparison of gaussian and mean curvatures estimation methods on triangular meshes. In *Proceedings of IEEE International Conference on Robotics and Automation*, volume 1, pages 1021–1026, Sept. 2003.

[28] G. Taubin. Estimating the tensor of curvature of a surface from a polyhedral approximation. In *Proceedings of the Fifth International Conference on Computer Vision*, pages 902–907, 1995.

[29] J. P. Thirion and A. Gourdon. Computing the differential characteristics of isointensity surfaces. *Computer Vision and Image Understanding*, 61(2):190–202, Mar. 1995.

[30] L. J. van Vliet, I. T. Young, and P. W. Verbeek. Recursive gaussian derivative filters. In *Proceedings of the 14th International Conference of Pattern Recognition (ICPR'98)*, pages 509–514, Aug. 1998.

[31] C. van Wijk, R. Truyen, R. E. van Gelder, L. J. van Vliet, and F. M. Vos. On normalized convolution to measure curvature features for automatic polyp detection. In *Medical Image Computing and Computer-Assisted Intervention MICCAI 2004 Part 1, Lecture Notes in Computer Science*, volume 3216, pages 200–208, Sept. 2004.

[32] V. Verma, D. Kao, and A. Pang. A flow-guided streamline seeding strategy. In *Proceedings of IEEE Visualization 2000 (VIS'00)*, pages 163–170, 2000.

[33] H. Yoshida, J. Näppi, P. MacEneaney, D. T. Rubin, , and A. H. Dachman. Computer-aided diagnosis scheme for detection of polyps at CT colonography. *Radiographics*, 22:963–979, 2002.